J. Fluid Mech. (1987), vol. 179, pp. 327–344
Printed in Great Britain

A model of interfacial stress and spray generation by gas flowing over a deep, wavy pool

By Y. L. SINAI
Research and Development, National Nuclear Corporation Limited,
Warrington Road, Risley, Warrington, Cheshire, WA3 6BZ, UK

(Received 10 March 1986)

A wave Reynolds number is the controlling parameter in Wang & Street's (1978) correlation for spray generation in developing air flow over a pool. A novel feature of the present theory is the prediction of the time-mean interfacial stress which, together with a wave-height correlation, is proposed and tested as a tool for quantifying that Reynolds number. The validation exercise shows that the results are generally acceptable, although the technique tends to underestimate the interfacial stress and droplet flux at high gas speeds. The analysis of experimental data has revealed some differences in the correlations which should be resolved.

1. Introduction

Liquid entrainment from a pool by gas flowing horizontally over its surface is a topic which manifests itself in wide-ranging branches of engineering and science. Examples relevant to the nuclear power industry concern, for instance, entrainment phenomena inside the primary pressure vessels of water-cooled reactors during postulated loss-of-coolant accidents. Entrainment from a contaminated pool, whether inside a vessel or building, or at a site exposed to the atmosphere, is of course important in the general safety-analysis area.

A literature survey has revealed that the majority of the relevant studies appear to have been conducted by oceanographers and civil engineers, motivated as they have been by the quest for an understanding of the influence of spray on ocean-atmosphere heat, mass and particulate transport, as well as on electromagnetic waves. Both field and laboratory studies have been reported (see, for example, Monahan 1968; Lai & Shemdin 1974; Wu 1973, 1979, 1982; Wang & Street 1978; Macha 1981). Of these works, only Lai & Shemdin (hereinafter referred to as LS), Wu, and Wang & Street (hereinafter referred to as WS) are in a form which can be exploited for predictive purposes. There are similarities between the three correlations, but the first two in fact quote measurements made at only one fetch, so Wang & Street's result emerges as the only candidate based on measurements in which both fetch and wind speed were varied. There are several misprints in WS, but these have been clarified in communications with Professor Street, and the correlation quoted in this paper is the correct one.

Pinchak (1966) presented an interesting study, but was limited by the assumptions of constant roughness or constant shear stress, as well as the absence of the experimental data alluded to above.

The salient features are sketched in figure 1. The pool is assumed to be deep, in the sense that the mean pool depth is much greater than the wavelength of any component of the surface gravity waves, so the work on entrainment in internal

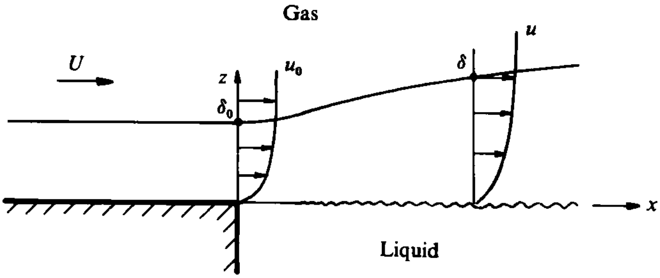

FIGURE 1. The pool problem.

film-annular flow (e.g. Cousins & Hewitt 1968; Hewitt & Hall-Taylor 1970; Zanelli & Hanratty 1971; Ishii & Grolmes 1975) is of limited value. It seems that four entrainment mechanisms have been observed (see figure 2).

(i) Tearing of liquid bulk. Here capillary (or roll) waves are torn or sucked away in regions of high shear (e.g. Hanratty & Woodmansee 1965; Brodkey 1967; Hewitt & Hall-Taylor 1970; Kataoka, Ishii & Mishima 1983).

(ii) Wave 'undercutting' in liquid films (e.g. Hewitt & Hall-Taylor 1970).

(iii) Splashing due to wave breaking and/or droplet impingement (e.g. Longuet-Higgins 1982; Nakagawa 1983).

(iv) Bubble bursting (Newitt, Dombrowski & Knelman 1954; Hewitt & Hall-Taylor 1970; Wu 1979; Coantic 1980; Longuet-Higgins 1983). As a bubble reaches a free surface, two droplet hierarchies arise. In the first, micrometre-sized 'film droplets' are produced by the disintegration of the dome of the bubble. The second hierarchy is a consequence of the vertical columnar jet produced by the inrush of liquid towards the centre of the crater which exists immediately after the bubble dome's demise; one or more droplets are produced, typically with diameters of several hundred micrometres. Bubbles are produced by splashing and/or boiling.

Droplet inception criteria originating in the studies of annular flows in tubes seem to over-predict the gas velocities, and this is probably directly attributable to the one major difference between the two cases, namely the role of gravity. The latter is responsible for wave breaking, splashing, gas entrainment into the liquid bulk and hence droplet production by bubble bursting, all at relatively low gas speeds. Indeed, water waves do not need an energy input from the wind in order to overturn and break, since non-linear effects can produce such phenomena, so that hydrodynamic events in the liquid can lead to wave breaking and splashing independently of the gas flow. Thus, breaking and droplet production can arise at low (or vanishing) gas speeds, and the question of droplet retention by the gas can simply depend on the competing roles of gas turbulence and gravitational settling. Be that as it may, Wang & Street derived a correlation for the droplet flux in terms of the Reynolds number:

$$R_\sigma = u_* \sigma / \nu_G,$$

where u_* is the gas friction velocity, σ is the r.m.s. interface elevation and ν_G is the gas kinematic viscosity. The correlation is based on air/water experiments, and all of the above-mentioned studies have indicated a droplet diameter spectrum which peaks in the region 150 to 200 micrometres. It is necessary to predict the interfacial stress and r.m.s. elevation before the WS correlation can be exploited.

The literature on transport across a sheared gas–liquid interface is extensive, particularly for turbulent flows (typical examples are Hanratty & Engen 1957;

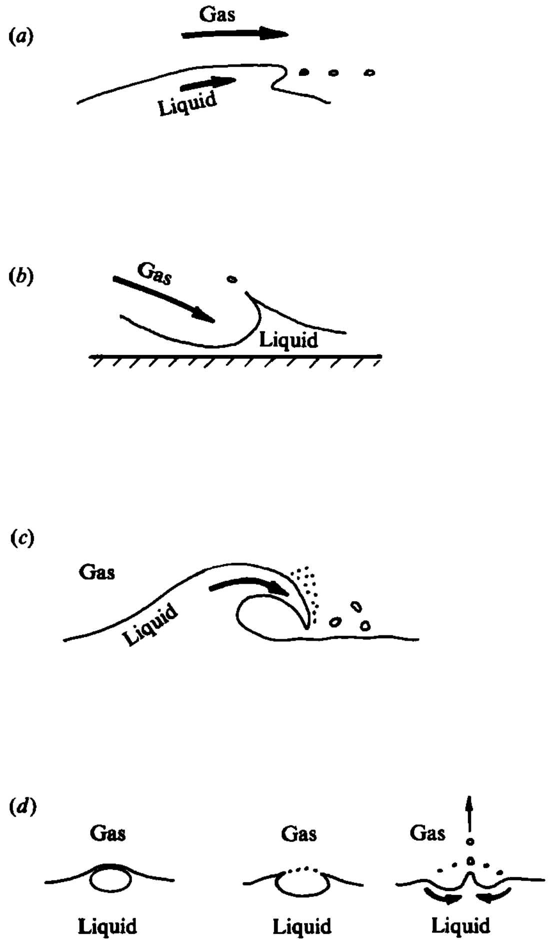

FIGURE 2. Droplet generation mechanisms: (a) shearing; (b) undercutting; (c) splashing; (d) bubble bursting.

Dukler 1972; Kotake 1974; Boyadjiev, Mitev & Bechkov 1976; Favre & Hasselman 1978; Street 1979; Coantic 1980; Jensen & Yuen 1982; Brutsaert & Jirka 1984). The transport of heat and mass across the interface has usually been characterized in terms of the friction velocity. In fully-developed conditions, oceanographers are able to predict u_* with a fair measure of confidence, given the wind speed at a certain reference height, as explained below. However, in a developing situation, such as flow over a liquid pool, there does not appear to be a method readily available for predicting the shear stress; the recent paper by Brighton (1985) is another example of the difficulties imposed by the absence of such a technique.

The pool problem (figure 1) is, in reality, an extremely complex one, involving liquid/gas coupling which depends on the geometry of the pool walls. Details of the geometry at the pool edge are clearly important, and the present study has assumed that at $x = 0$ the liquid is still, smooth and exactly flush (viz. at $z = 0$) with the flat wall existing in $x < 0$. The laminar version of the problem has recently been addressed by Clarke (1985). The problem bears some resemblance to the flow of a turbulent boundary layer acros a step change in roughness (e.g. Elliott 1958; Townsend 1965; Antonia & Luxton 1971; Nikitin 1972; Deaves 1981; Hunt & Simpson 1982; Wood

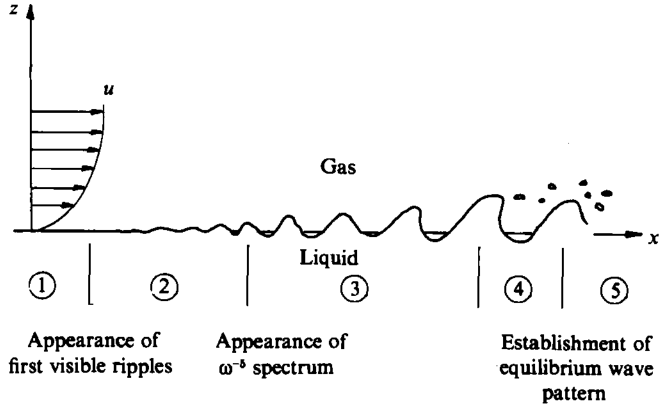

FIGURE 3. Sketch of the evolution of wind waves with distance, after Plate (1978). Region 1: No visible disturbance. Region 2: Linear growth, constant mean frequency ω and wavelength λ. Region 3: Non-linear growth, ω decreases with x, λ increases with x. Region 4: Wave breaking, appearance of significant concentrations of bubbles and droplets. Region 5: Dynamic equilibrium.

1982), with one crucial difference: in the present case the roughness along the interface is not fixed, but rather variable and, indeed, coupled to the gas flow. The gas and liquid flows are effectively uncoupled in this paper by exploiting an hypothesis, named after Charnock and widely used in oceanography (Charnock 1955; Hsu 1974; Phillips 1977; Wengefeld 1978; Wu 1980), which states that the aerodynamic roughness ϵ is proportional to u_*^2/g. Sinai (1983*a*, *b*, 1986*a*, *b*) has shown that Charnock's relation can be applied successfully to internal, fully-developed, stratified two-phase flows, and extended its use to cover other gas–liquid pairs provided their ratio of densities is small. The present theory generalizes that approach to the slowly developing situation with negligible pressure gradient, as in a flat-plate boundary layer. It would best be categorized as a gross momentum-integral method, since the upstream boundary layer is assumed to be thin on a macroscopic scale and the detailed development of the internal boundary layer is ignored. Such simple modelling incurs some penalties, of course, but these are outweighed by several advantages, including a universal first-order differential equation which is easily integrated numerically, an algebraic friction law valid far from the pool leading edge (Sinai 1982), and surprisingly good agreement with experiments.

It now only remains to calculate the r.m.s. interface displacement $\sigma(x)$. However, water-wave generation by wind is a substantial subject in its own right which has occupied many researchers over a period spanning most of this century. This paper gives only a brief outline, for further details see, for example, Ursell (1956), Kinsman (1965), Kitaigorodskii (1973), Phillips (1977), Favre & Hasselmann (1978), Hsu *et al.* (1982) and Ewing (1983). The steady-state pool problem involves spatial, rather than temporal instabilities, and (see figure 3) researchers have identified five domains. In region 1 there are no noticeable disturbances. In region 2, the first visible ripples appear. Their cause is still a contentious issue; one possibility links the ripples to the coherent structures which have aroused so much interest in recent years (e.g. Cantwell 1981). This region is described by linear instability where the dominant frequency in the wave spectrum remains constant but the corresponding wave amplitude grows exponentially. Apparently, existing theories do not compare too well with experiment, although it should be noted that the experiments are notoriously difficult to carry out; classical Kelvin–Helmholtz instability fares worst, and the three commonest theories are those attributable to Jeffreys, Miles and Phillips (see references above). Region 3 is one of nonlinear growth in which the dominant wavelength increases and the amplitude increase is slower than exponential. In region 4 the two phases begin to mix, with the appearance of significant quantities of bubbles and droplets. Dynamic equilibrium is established in region 5. Since there are no techniques available for predicting the sizes of the first four domains, and in view of the manifest complexity, a well-tested correlation, quoted in the book by Phillips (1977), has been used and modified slightly in this paper to complete the calculation of R_σ and hence the droplet flux.

Finally, this paper concludes with a few comments on the calculation of pool entrainment from a bubbling or boiling pool. The term 'pool entrainment' is conventionally interpreted as liquid entrainment by gas flowing vertically through the pool, as occurs in evaporators, fluidized beds, steam generators, and light-water reactors' core reflood. The real behaviour is more complex since it is a combination of both types of entrainment – by gas flowing over *and* through the pool (when the latter is bubbling), but in this paper the two mechanisms are considered to be independent. Of the early literature on conventional pool entrainment, the papers by Garner, Ellis & Lacey (1954) and Newitt *et al.* (1954) are notable; a review and extension of modern approaches may be found in Kataoka & Ishii (1984).

2. Boundary-layer similitude and the variation of Charnock's parameter

The momentum-integral theory delineated in this report is based, as is customary, on a similarity law for the local velocity profile, and the following form is one which encompasses arbitrary roughness as well as a velocity-defect law:

$$\frac{u}{u_*} = \frac{1}{K}\left[\ln\left(\frac{z}{\epsilon}\right) + \Psi\right], \tag{2.1}$$

$$\Psi(R_\epsilon, \eta) = K\hat{B}(R_\epsilon) + h(\eta), \quad \eta = \frac{z}{\delta}, \quad R_\epsilon = \frac{u_* \epsilon}{\nu_G}. \tag{2.2}$$

Here $\hat{B}$ is the roughness function (e.g. Pai 1957; Schlichting 1960; Goldstein 1965), K is von Kármán's constant (≈ 0.4), h is the velocity-defect component and δ is the boundary-layer thickness. Coles' Law of the Wake is widely used (e.g. Tennekes & Lumley 1972), and for small pressure gradients this reads

$$h(\eta) = 0.55\{1 + \sin[\pi(\eta - \tfrac{1}{2})]\}. \tag{2.3}$$

The roughness function $\hat{B}$ attains the following asymptotic forms.

(i) As $R_\epsilon \rightarrow 0$ (smooth flow), $\hat{B} \sim K^{-1}\ln(9R_\epsilon)$.

(ii) As $R_\epsilon \rightarrow \infty$ (fully-rough flow), $\hat{B} \sim K^{-1}\ln(30)$.

In intermediate domains the behaviour of $\hat{B}$ is not necessarily monotonic and depends on the detailed roughness geometry, viz. shape and spacing. For a liquid/gas interface it would be impossible to specify detailed roughness geometry, and therefore a convenient composite form, mimicking the cardinal features of $\hat{B}$, has been assumed:

$$\hat{B}(R_\epsilon) = \frac{-1}{K}\ln\left(\frac{1}{30} + \frac{1}{9R_\epsilon}\right). \tag{2.4}$$

This relation is monotonic in R_ϵ. Equation (2.1) is now rewritten as

$$u = \frac{u_*}{K}\ln\left(\frac{z}{\alpha}\right), \tag{2.5}$$

$$\alpha(\epsilon, u_*, \eta) = \epsilon \exp(-\Psi). \tag{2.6}$$

When (2.4) is invoked

$$\alpha(\epsilon, u_*, \eta) = \gamma \exp(-h), \tag{2.7}$$

$$\gamma(\epsilon, u_*) = \frac{\epsilon}{30} + \frac{\nu_G}{9u_*}. \tag{2.8}$$

The quantity γ is the generalized roughness length. In essence, (2.4) is equivalent to the Colebrook–White empiricism of flow resistance in conduits (e.g. Streeter & Wylie 1979), although in the present analysis the roughness ϵ is permitted to depend on the gas flow.

As regards the roughness, Charnock's relation, which states that the roughness ϵ is proportional to u_*^2/g, has already been mentioned in §1, and the reader is referred to the material listed there for additional details.

Oceanographers have concentrated on 'saturated' (viz. fully-developed) conditions and air-freshwater or air/saltwater as the operating fluids, and the Charnock constant $\hat{\mu}$ has been defined by

$$\epsilon = \frac{\hat{\mu} u_*^2}{g}. \tag{2.9}$$

There is considerable discussion in the literature on the value of $\hat{\mu}$ (Hsu 1974; Phillips 1977; Wu 1980) but without being drawn into a detailed appraisal of experimental variations and measurement techniques, the apparently common value of about 0.33 will be accepted here. Sinai (1983*a*) has allowed for fluids other than air and water at normal conditions by writing

$$\epsilon = \frac{\mu \xi u_*^2}{g}, \quad \mu \approx 275, \quad \xi = \frac{\rho_G}{(\rho_L - \rho_G)}. \tag{2.10}$$

Effectively, (2.10) reflects a balance between the stress $\rho_G u_*^2$ tending to disrupt the interface and the buoyancy $(\rho_L - \rho_G)g$ tending to stabilize the stratified structure. The value of μ given here appertains to developing (internal or external) and fully-developed external flows.

Next, Charnock's relation is generalized to developing flows by assigning a prescribed variation with x of μ. The model, sketched in figure 4, is based on the paper by Shaw & Lee (1976), where several laboratory experiments were scrutinized; great accuracy cannot be expected from the present techniques, and the model is therefore proposed as a universal function valid for any situation except thin liquid films and mechanically-generated waves. The function is

$$\mu = \begin{cases} x(183.3 - 30.56x) & (x \leqslant 3 \text{ metres}), \\ 275 & x > 3 \text{ metres}. \end{cases} \tag{2.11}$$

The quantity μ is dimensionless, but the distance x appearing in (2.10) must be expressed in metres. The adopted model benefits from the appealing feature of vanishing roughness at $x = 0$, which helps to overcome the mathematical and physical difficulties encountered in the fully-rough theory (Sinai 1982) in relation to the initial conditions (cf. §3).

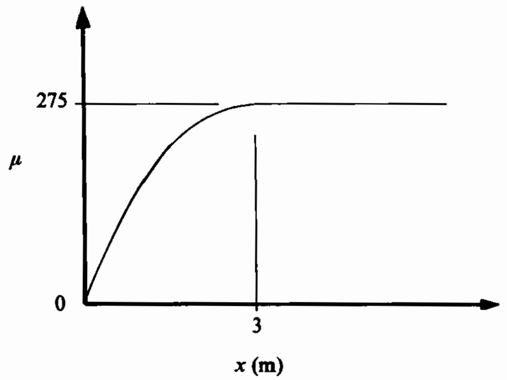

FIGURE 4. Sketch of the adopted Charnock parameter. The relation is given by (2.11).

3. A momentum-integral calculation of interfacial stress and comparisons with experiments

As explained in §1, the present theory is based on the neglect of details of the development of the inner boundary layer (cf. figure 1), so that the integral equation (e.g. Elliott 1958), valid for laminar and turbulent boundary layers with negligible pressure gradient, is simplified to the classical form (e.g. Schlichting 1960; Goldstein 1965)

$$U^2 \frac{\mathrm{d}\delta_2}{\mathrm{d}x} = u_*^2. \tag{3.1}$$

Here U is the free-stream velocity (assumed constant), u_* is the friction velocity $(\tau/\rho_G)^{\frac{1}{2}}$, τ is the time-mean surface shear stress, ρ_G is the gas density, and δ_2, δ are the momentum and boundary-layer thicknesses respectively:

$$\delta_2 = \int_0^\delta \frac{u}{U}\left(1-\frac{u}{U}\right)\mathrm{d}z. \tag{3.2}$$

Essentially, this is the approach investigated previously by Sinai (1982), although certain mathematical and physical obstacles in that work have been overcome by introducing two refinements.

(i) Charnock's constant is allowed to vary with distance.

(ii) Molecular viscosity is included, thereby removing the constraint confining the layer air flow to be fully rough (Schlichting 1960; Goldstein 1965) everywhere above the interface.

Charnock's relation, or rather its adapted form, encapsulates the coupling between gas and liquid, and its adoption conveniently uncouples the equations of motion for the two fluids. Thus, given a free-stream velocity U and the gas physical properties, (3.1) is a first-order differential equation for boundary-layer flow over a surface the roughness of which depends on the local (unknown) shear stress.

Initially, the procedure for determining u_* closely follows the classical von Kármán method (Goldstein 1965). The similarity law for turbulent flow, equation (2.1), is expressed as

$$u = U - u_* f(\eta), \quad \eta = \frac{z}{\delta},$$

$$f(\eta) = \frac{-1}{K}[\ln(\eta) + h(\eta) - h(1)]. \tag{3.3}$$

From the definition of δ_2 (equation (3.2)),

$$\delta_2 = \frac{u_* \delta}{U}\left(C_1 - C_2 \frac{u_*}{U}\right),$$

$$C_1 = \int_0^1 f(\eta)\,\mathrm{d}\eta, \quad C_2 = \int_0^1 f^2(\eta)\,\mathrm{d}\eta. \tag{3.4}$$

From equations (2.5) and (2.7) it follows that

$$U = \frac{u_*}{K}\ln\left(\frac{\beta\delta}{\gamma}\right), \quad \beta = \exp[h(1)]. \tag{3.5}$$

The analysis is now expedited by introducing a new dependent variable

$$\Delta = \ln\left(\frac{\beta\delta}{\gamma}\right), \quad \delta = \frac{\gamma \exp(\Delta)}{\beta}. \tag{3.6}$$

Then (3.5) becomes

$$\frac{u_*}{U} = \frac{K}{\Delta}. \tag{3.7}$$

Invoking the modified Charnock relation (equations (2.10), (2.11)) and the generalized roughness length (equation (2.8)),

$$\left.\begin{aligned} \gamma &= \frac{A\mu}{\Delta^2} + B\Delta, \\ A &= \frac{\xi K^2 U^2}{30g}, \quad B = \frac{\nu_G}{9KU}. \end{aligned}\right\} \tag{3.8}$$

Define a non-dimensional distance X by

$$X = x/A. \tag{3.9}$$

Substitution in (3.1) then leads, after some algebra, to the following first-order, ordinary differential equation for Δ:

$$G\frac{\mathrm{d}\Delta}{\mathrm{d}X} = H, \tag{3.10}$$

$$G = D(C_1\Delta^5 - M\Delta^4 + M\Delta^3) + \mu[C_1\Delta^2 - (3C_1 + M)\Delta + 4M], \tag{3.11}$$

$$H = \Delta\left[K\beta\Delta^2 \exp(-\Delta) + \frac{\mathrm{d}\mu}{\mathrm{d}X}(M - C_1\Delta)\right], \tag{3.12}$$

$$D = B/A, \quad M = KC_2. \tag{3.13}$$

There are two interesting limits which can be usefully checked:

(i) Zero roughness. Here $\mu = 0 = \mathrm{d}\mu/\mathrm{d}x$, and (3.10) becomes

$$(C_1\Delta^2 - M\Delta + M)\,\mathrm{e}^{\Delta}\frac{\mathrm{d}\Delta}{\mathrm{d}X} = \frac{9K^2\beta UA}{\nu_G}, \tag{3.14}$$

which is identical to the classical smooth-plate equation (Goldstein 1965).

(ii) Fully-rough flow with constant Charnock parameter.

This is the situation addressed previously (Sinai 1982) and should be derived from (3.10) by letting B and $\mathrm{d}\mu/\mathrm{d}x$ tend to zero:

$$[C_1\Delta^2-(3C_1+M)\Delta+4M]\frac{\mathrm{e}^{\Delta}}{\Delta^3}\frac{\mathrm{d}\Delta}{\mathrm{d}X}=\frac{K\beta}{\mu}. \tag{3.15}$$

This equation has the following closed-form solution:

$$\frac{\beta KX}{\mu}=(3C_1-M)\left(\frac{\mathrm{e}^{\Delta}}{\Delta}-\frac{\mathrm{e}^{\Delta_0}}{\Delta_0}\right)-2M\left(\frac{\mathrm{e}^{\Delta}}{\Delta^2}-\frac{\mathrm{e}^{\Delta_0}}{\Delta_0^2}\right)+(M-2C_1)\,[\mathrm{Ei}(\Delta)-\mathrm{Ei}(\Delta_0)] \tag{3.16}$$

where Ei is the exponential integral (Abramowitz & Stegun 1972) and Δ_0 is the value of Δ at $x=0$. In fact, it can be seen from (3.6) that a value can be assigned to Δ_0 iff:

$$\delta_0>\frac{0.25e^2\mu A}{\beta}. \tag{3.17}$$

This condition is related to the existence of solutions to the formula used in oceanography (e.g. Phillips 1977),

$$u_*^2\exp\left(\frac{Ku}{u_*}\right)=\frac{30gz\beta}{\mu\xi}, \tag{3.18}$$

where the reference height z is normally chosen to be 10 m and u is the velocity at that height. This may be seen by noting that in the present case, the relation between δ and Δ (or equivalently u_*/U), equation (3.6), reads

$$\exp(\Delta)-\left(\frac{\delta}{A\mu}\right)\Delta^2=0.$$

Regarding this expression as an equation for Δ with $\delta/A\mu$ as a parameter, it immediately follows that two solutions exist if (3.17) is satisfied, and it is the larger of the two solutions which is pertinent, since the smaller Δ_0 would lead to a boundary layer the thickness of which decreases with distance. At the minimum conditions, when the two solutions coalesce, $\Delta=2$ and $\beta\delta/\gamma=e^2\approx 7.4$, or $\delta/\epsilon\approx 0.1$ since β is close to e. Thus, values of Δ which are close to 2 are unphysical because they imply a boundary-layer thickness which is comparable to or less than the physical roughness height.

Equation (3.18) has no solution if

$$\frac{30gz\beta}{\mu\xi K^2U^2}<0.25e^2. \tag{3.19}$$

In the oceanographic context, this requires the velocity at 10 m to be over 600 km/h, and it is difficult to assign a physical meaning to such a condition, but Sinai (1983*a*) has shown that the mathematical breakdown does have physical significance for internal two-phase flows, where it corresponds to the transition from the stratified to the slug regimes.

The complete modelling embodied in (3.11), which accounts for molecular viscosity and vanishing roughness at the origin, does not suffer from these shortcomings with relation to the initial conditions. Nevertheless, it is interesting to proceed with an evaluation of the asymptotic behaviour of (3.16) far downstream, where the friction coefficient is small and Δ is large.

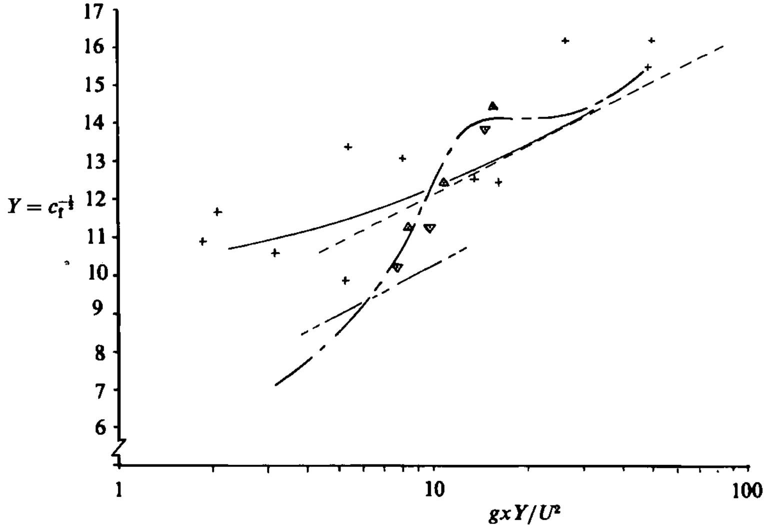

FIGURE 5. Comparison of experimental data for interfacial stress with the asymptotic theory. ––––– Wu (1968); △, Lai & Shemdin (1978), $x = 24.4$ m, freshwater; ▽, Lai & Shemdin, saltwater; +, Hidy & Plate (1966); –·–·–, Street *et al.* (1978), $x = 10.5$ m; ——, full theory, $x = 10.5$ m, equation (3.10); ----, asymptotic theory $h = 0$, equation (3.22).

It can be shown that when Δ is large it is given simply by

$$C_1 \Delta^{-1} \exp(\Delta) \sim \frac{\beta K x}{A\mu}. \tag{3.20}$$

In terms of the more familiar friction coefficient, defined as

$$c_f = 2\left(\frac{u_*}{U}\right)^2 = \frac{2K^2}{\Delta^2}, \tag{3.21}$$

the above equation can be written as

$$\frac{1}{c_f^{\frac{1}{2}}} = \frac{1}{2^{\frac{1}{2}}K} \ln\left(\frac{30\sqrt{2}\beta}{\mu\eta C_1}\right) + \frac{1}{2^{\frac{1}{2}}K} \ln\left(\frac{x}{\hat{\epsilon} c_f^{\frac{1}{2}}}\right), \tag{3.22a}$$

where

$$\hat{\epsilon} = U^2/g. \tag{3.22b}$$

It is worthwhile comparing this result with the classical rough-plate relation (e.g. Schlichting 1960; Goldstein 1965):

$$\frac{1}{c_f^{\frac{1}{2}}} = \frac{1}{2^{\frac{1}{2}}K} \ln\left(\frac{30\beta}{2^{\frac{1}{2}}C_1}\right) + \frac{1}{2^{\frac{1}{2}}K} \ln\left(\frac{x c_f^{\frac{1}{2}}}{\epsilon}\right), \tag{3.23}$$

where ϵ is the fixed roughness height. The latter equation always possess a solution, but (3.22*a*) has no solution when $\Delta < 1$, which is a condition analogous to (3.19). Examination of the algebraic structure of (3.22*a*) shows that when $\Delta > 1$, two solutions exist. One implies that c_f increases with x and decreases with U, which is deemed unrealistic, and a second which predicts c_f decreasing with x and increasing with U (see Wu 1980).

Figure 5 presents a comparison between (3.22) (assuming $h = 0$), the full numerical solution of (3.10) for a specific fetch x, and experimental data of Hidy & Plate (1966),

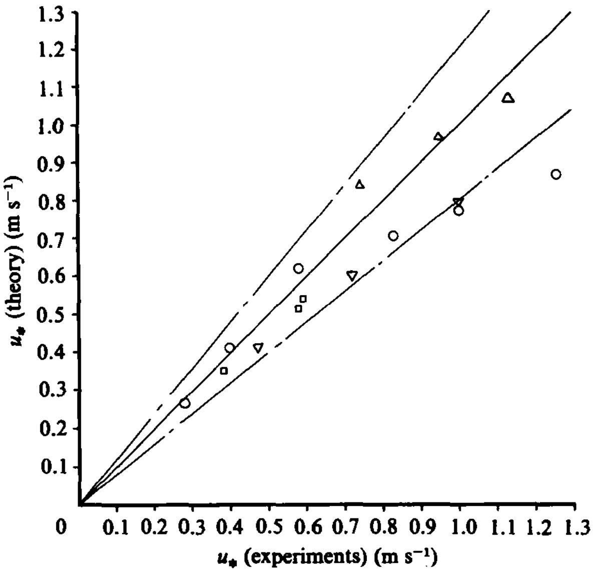

FIGURE 6. Interfacial stress: Comparison of theory (equation (3.10)) with experiment. ○, Street *et al.* (1978); □, Street (1979); △, Lai & Shemdin (1974); ▽, Wu (1968). Theory assumed $h = 0$.

Wu (1968), Lai & Shemdin (1974) and Street *et al.* (1978). Sinai (1986*c*) gives further discussion of this case.

Turning now to the full equation (3.10), it has been integrated numerically and compared with experimental data. The predictions of interfacial stress are good, as shown in figure 6, although the theory underpredicts u_* when the observed value is greater than about 1.2 m s^{-1}.

As regards the r.m.s. wave height σ, Phillips (1977) quotes a correlation which predicts $\sigma \propto u_*(x/g)^{\frac{1}{2}}$. However, comparison with the experimental data considered in this paper indicates a consistent underprediction by that correlation, and far better agreement has been obtained by increasing the constant of proportionality by 40 %, provided the local values of u_*, as predicted by (3.10) are used:

$$\sigma = 0.0178 u_* \left(\frac{x}{g}\right)^{\frac{1}{2}}. \tag{3.24}$$

This difference is probably attributable to discrepancies in scale; the correlation as given by Phillips has been applied to fetches of tens to hundreds of kilometres (with minor variations in u_*), whereas the present paper is concentrating on experimental data covering distances of up to several tens of metres. As shown in figure 7, (3.24) is quite successful (mechanically generated waves are excluded).

Some feel for the influence of upstream conditions on the interfacial stress can be gleaned from figure 8, which shows the evolution of u_* for two values of c_{f_0}. Predictably, the effects are significant at relatively small distances and diminish with increasing x, but it should be remembered that the present analysis is not expected to be accurate near the origin because it ignores the details of the inner layer.

It is also interesting to examine the ratio of roughness ϵ to r.m.s. wave height σ (see figure 9), since it reflects the point made by Wu (1980), that the roughness can usually be related to the significant waves themselves in the laboratory and to the small-scale waves in field conditions. Street (1979) reports that for the Stanford

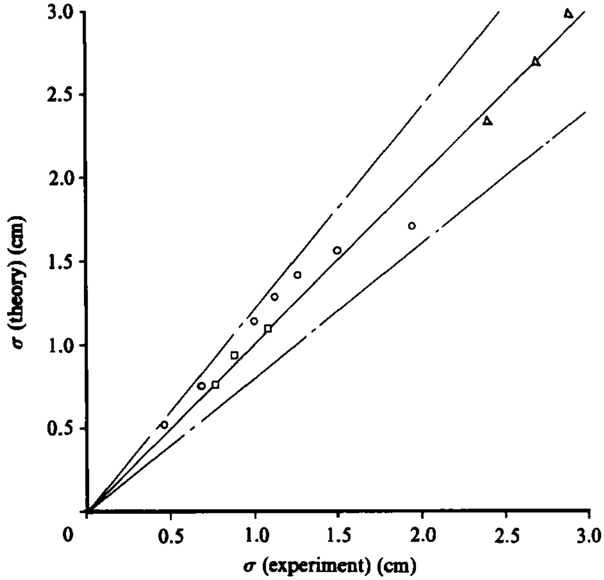

FIGURE 7. R.m.s. wave height: Comparison of theory (equations (3.10) and (3.24) *vs.* experiment. ○, Street *et al.* (1978); □, Street (1979); △, Lai & Shemdin (1974).

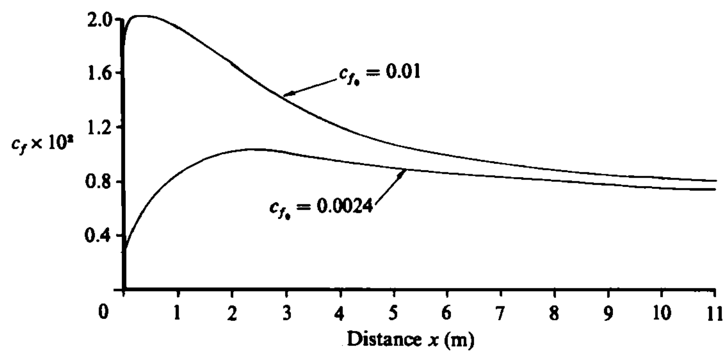

FIGURE 8. An example of the influence of upstream conditions. $U = 14.5$ m s^{-1}, $h = 0$.

wind–water facility the roughness is about 2.5σ, and in §4 we shall emphasize the differences between the WS spray measurements and those of Lai & Shemdin (1974), taken at larger fetch where ϵ/σ was significantly smaller than 2.5. Figure 9 shows ϵ/σ versus x for $U = 10$ and 14.5 m s^{-1}, and it illustrates the decay of this ratio for large x,

$$\frac{\epsilon}{\sigma} \propto x^{-0.61}. \tag{3.25}$$

This relation, taken together with (2.9) and (3.24) implies that u_* decays slowly, as $x^{-0.11}$. There are slight differences between the decay exponents at the two speeds, and for present purposes the value in (3.25) may be taken as -0.61 ± 0.01.

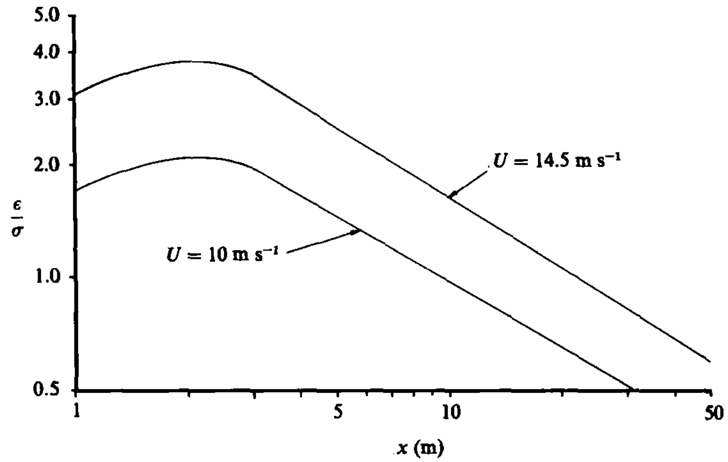

FIGURE 9. Predicted ratio of roughness to r.m.s. wave height *vs.* fetch. $c_{f_0} = 0.0024$.

4. Entrainment predictions and validation

As discussed in §1, Wang & Street's (1978) correlations are considered here to be the most versatile since, unlike the other studies, both the wind speed and the distance were varied. However, it will be shown below that some reservations have to be made with regard to all the laboratory-based correlations.

The WS formulae consist of two steps. The first defines the height of the droplet layer above which the aerosol concentration is effectively zero, in terms of the wave height and friction velocity:

$$R_\mathrm{d} = 19.4R_\sigma - 6000, \tag{4.1a}$$

where

$$R_\sigma = \frac{u_* \sigma}{\nu}, \quad R_\mathrm{d} = \frac{u_* z_\mathrm{d}}{\nu}. \tag{4.1b}$$

Here z_d is the droplet-layer height, and ν is the gas kinematic viscosity. Equation (4.1*a*) is the corrected form of the WS relation, as confirmed in communications with Professor Street. The final step relates the droplet flux (passing through the vertical plane) to z_d,

$$\frac{n}{n_*} = K^{-1} \ln\left(\frac{z_\mathrm{d}}{z}\right), \tag{4.2}$$

$$n_* = 1.3 \exp(1.25 \times 10^{-4} R_\mathrm{d})\ \mathrm{cm^{-2}\ s^{-1}}. \tag{4.3}$$

The results of computations using (3.10) and (4.1)–(4.3) are shown in figure 10, for conditions appertaining to the WS experiments. Unfortunately, none of the studies reported details of the upstream conditions, and the present computations have utilized the standard Blasius correlation to estimate c_{f_0}, assuming a distance of 7.5 m between the facility's air inlet and the water's edge. It seems that the theory is reasonably successful up to speeds of about 14 m $\mathrm{s^{-1}}$, but it underestimates the droplet flux significantly above that speed. However, an important point to note is that the velocity U quoted by the experimentalists has invariably been a 'reference' velocity which is not necessarily the 'free-stream' velocity assumed here. Ideally, the experimental data should have included detailed information on conditions of the flow approaching the pool.

Examination of the results shows that the discrepancies at higher gas speeds are

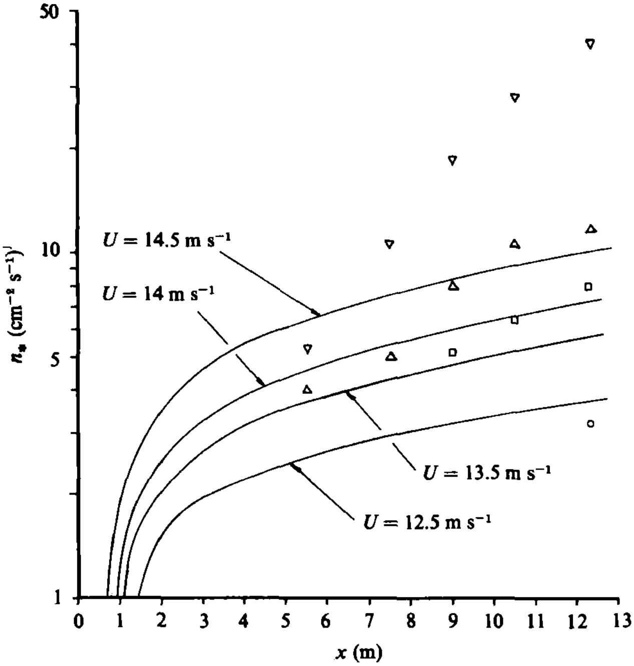

FIGURE 10. 'Friction' droplet flux: Theory and experiment *vs.* fetch. Experiment Wang & Street (1978): ○, $U = 12.5$ m s^{-1}; □, $u = 13.5$ m s^{-1}; △, $U = 14.0$ m s^{-1}; ▽, $U = 14.5$ m s^{-1}; ——, theory.

Run	U_{ref} (m s^{-1})	R_σ (expt)	R_σ (theory)	R_d (expt)	R_d (theory)	n_* (expt)	n_* (equation (4.3))
4	15.0	1.32×10^3	1.40×10^3	1.00×10^4	2.12×10^4	1.4	19
5	16.7	1.91×10^3	1.87×10^3	1.52×10^4	3.02×10^4	6.8	57
6	18.0	2.45×10^3	2.27×10^3	2.13×10^4	3.80×10^4	14	151

TABLE 1. Lai & Shemdin data and predictions

attributable to an underestimation of u_* and to the sensitivity (due to the exponential form) of n_* thereto (note that in the present framework R_σ is proportional to the square of u_*). However, several important conclusions can be deduced if comparisons are made with data from different experimental rigs. For example, figures 6 and 7 show that whereas (3.10) and (3.24) underestimate u_* and σ when compared with the Stanford University data for $U \geqslant 14$ m s^{-1}, the predictions of those quantities are gratifying when compared with Lai & Shemdin's data for the University of Florida facility at speeds of 15.0, 16.7 and 18.0 m s^{-1}. This indicates that the laboratory studies may not necessarily provide data which can be applied to the behaviour of a pool exposed to the atmosphere, for example. This view is reinforced when the LS spray data are scrutinized. Consider the data for the freshwater tests without mechanically generated waves (little difference was observed by LS between freshwater and saltwater spray concentration), runs 4, 5 and 6 (table 1).

Interpretation of these numbers immediately shows that the discrepancies are due to differences in the values of R_d, and more specifically, since the present theory compares very well as regards u_*, due to differences in the droplet-layer height z_d. Indeed, Wang & Street presented a comparison of their data and correlation with the LS data which indicated good agreement (their figure 7). However, that evaluation only checked the relation between n_* and R_d, and the present comparisons show that equation (4.1*a*) predicts values of R_d which are about double those measured by Lai & Shemdin.

There are several candidate explanations for the discrepancies in z_d:

(i) The aerodynamic and hydrodynamic characteristics of the various facilities are certainly not identical. Some facilities possess a roof over the whole channel, whereas others have a roof running over only part thereof. The University of Florida facility has an air intake designed to simulate rough turbulent air flow, whereas the other rigs do not. The sketches of the geometrical features in the published papers are vague about the details of the manner in which the air flow merges with and contacts the water bulk; for example, in two sketches of the same facility, one showed the lower lip of the air inlet ducting apparently touching the water surface at $x = 0$, whereas the other showed the lip displaced well above the water surface, and such features must surely influence the evolution of the interface.

(ii) Different techniques were used for measuring the spray concentrations and size spectra. Wu (1973) used a laser and phototransistor, Lai & Shemdin (1974) used a hot-film anemometer and Wang & Street (1978) used an electrostatic capacitance wire probe. The author is not qualified to comment on the relative merits of the various methods, but it seems that these doubts would only be resolved by testing these systems at one facility and under identical conditions.

Summarizing, it appears that whilst (4.3) has been found to be generally realistic, the WS correlation between droplet-layer height and wave Reynolds number, (4.1), must be used with caution since it conflicts with measurements made by other workers. Care must also be taken not to extrapolate (4.3) much beyond values of $R_d = 4 \times 10^4$ since the exponential form only describes the explosive growth of droplet concentration under conditions which are likely to arise in the atmosphere (see Wu 1973).

5. Conclusions

By modelling observed variations of Charnock's parameter (in developing flows), relating the aerodynamic roughness to interfacial stress, it has been possible to decouple the gas and liquid flows in the pool problem and to determine the interfacial drag after a single numerical integration of a generalized boundary-layer equation (3.10). The asymptotic behaviour of that equation has been evaluated (equation (3.22)). When the computations are combined with an empirical correlation for wave excitation by wind, one can determine the wave Reynolds number R_σ which is the controlling parameter in correlations for spray production by air flowing over water (Wang & Street 1978). Comparison of the theory with measurements of stress and wave height has been surprisingly favourable, despite the crude assumptions underlying the method, although (3.10) tends to underestimate u_* for the Stanford facility at reference air speeds greater than 14 m s^{-1}.

An exercise intended to validate the predictive technique has revealed significant differences between the droplet-layer behaviour reported for the Florida (Lai & Shemdin 1974) and Stanford (Wang & Street 1978) facilities; possible explanations are suggested in §4. Thus, it appears that whilst the gross theory presented in this paper is capable of predicting u_* and σ with acceptable accuracy, (4.1*a*) must be treated with caution, and moreover, (4.3) is extremely sensitive to variations in the product of u_* and σ. Nevertheless, the method is a useful tool in a field where, so far, no previous calculations have been proffered.

The above procedure applies to entrainment from a pool, the bulk of which is devoid of gas or vapour. If, however, the pool is bubbling or boiling, a conservative (viz. maximum likely) estimate of this contribution can be made with the correlations proposed by Kataoka & Ishii (1984). The behaviour of the interface under the combined actions of a horizontal wind above and bubbles approaching from below is extremely complex and merits further investigation.

Kataoka and Ishii point out that in the near-surface region some of the drops are large, and short-lived in the usual pool situation, but if high horizontal gas flows arise above the fluid one may assume initially that the complete spectrum of sizes is carried away. Whilst bubble bursting would roughen the free surface, the wind-generated waves would tend to destroy the efficiency of the columnar-jet process of droplet generation by bubble bursting, and it is not obvious whether, under combined conditions of wind and bubbling, the droplet source will be less or greater than the simple sum of the two contributions.

As regards fluid pairs other than air and water, the model of interfacial stress proposed herein is a fairly general one, but the correlations for wave height and droplet flux are not expected to succeed for fluids possessing physical properties which differ significantly from those of air and water.

I wish to acknowledge the assistance of the Marine Information and Advisory Service of the Institute of Oceanographic Sciences for its support with the literature survey. Professor R. L. Street helped to clarify the correlations which appeared in the WS paper. I also wish to thank the staff at the NNC library and General Editorial Department. This paper is published by permission of the National Nuclear Corporation.

REFERENCES

ABRAMOWITZ, M. & STEGUN, I. A. 1972 *Handbook of Mathematical Functions*. Dover.

ANTONIA, R. A. & LUXTON, R. E. 1971 The response of a turbulent boundary layer to a step change in surface roughness. Part 1. Smooth to rough. *J. Fluid Mech.* **48**, 721–761.

BOYADJIEV, C., MITEV, P. & BECHKOV, V. 1976 Laminar boundary layers at a moving interface generated by a counter-current gas–liquid stratified flow. *Intl J. Multiphase Flow* **3**, 61–66.

BRIGHTON, P. W. M. 1985 Evaporation from a plane liquid surface into a turbulent boundary layer. *J. Fluid Mech.* **159**, 323–345.

BRODKEY, R. S. 1967 *The Phenomena of Fluid Motion*. Addison-Wesley.

BRUTSAERT, W. & JIRKA, G. H. (ed.) 1984 *Gas Transfer at Water Surfaces*. Reidel.

CANTWELL, B. J. 1981 Organised motion in turbulent flow. *Ann. Rev. Fluid Mech.* **13**, 457–515.

CHARNOCK, H. 1955 Wind stress on water surface. *Q. J. R. Met. Soc.* **81**, 639.

CLARKE, D. 1985 Problems in triple-deck boundary layer theory. Ph.D. thesis, Department of Mathematics, University of Manchester.

COANTIC, M. 1980 Mass transfer across the ocean–air interface: Small scale hydrodynamic and aerodynamic mechanisms. *Physico-Chemical Hydrodyn.* **1**, 249–279.

COUSINS, L. B. & HEWITT, G. F. 1968 Liquid phase mass transfer in annular two-phase flow: Droplet deposition and liquid entrainment. *AERE*-R5657.

DEAVES, D. M. 1981 Computations of wind flow over changes in surface roughness. *J. Wind Engng & Ind. Aerodyn.* **7**, 65–94.

DUKLER, A. E. 1972 Characterisation effects and modelling of the wavy gas–liquid interface. Proc. Intl Symp. on Two-phase Systems, Haifa (1971). *Prog. Heat Mass Transfer* **6**, 207–234.

ELLIOTT, W. P. 1958 The growth of the atmospheric boundary layer. *Trans. Am. Geophys. Union* **39**, 1048–1058.

EWING, J. A. 1983 Wind waves: A review of research during the last twenty-five years. *Geophys. J. R. Astr. Soc.* **74**, 313–329.

FAVRE, A. & HASSELMANN, K. 1978 *Turbulent Fluxes Through the Sea Surface, Wave Dynamics and Prediction.* Plenum.

GARNER, F. H., ELLIS, S. R. M. & LACEY, J. A. 1954 The size distribution and entrainment of droplets. *Trans. Instn Chem. Engrs* **32**, 222–235.

GOLDSTEIN, S. 1965 *Modern Developments in Fluid Dynamics.* Dover.

HANRATTY, T. J. & ENGEN, J. M. 1957 Interaction between a turbulent air stream and a moving water surface. *AIChE J.* **3**, 299–304.

HANRATTY, T. J. & WOODMANSEE, D. E. 1965 Stability of the interface for a horizontal air–liquid flow. *Symp. on Two-Phase Flow, Exeter, June 1965*, Paper A1.

HEWITT, G. F. & HALL-TAYLOR, N. S. 1970 *Annular Two-phase Flow.* Pergamon.

HIDY, G. M. & PLATE, E. J. 1966 Wind action on water standing in a laboratory channel. *J. Fluid Mech.* **26**, 651–687.

HSU, C.-T., WU, H.-Y. & STREET, R. L. 1982 Momentum and energy transfer in wind generation of waves. *J. Phys. Oceanogr.* **12**, 929–951.

HSU, S. A. 1974 A dynamic roughness equation and its application to wind stress determination at the air–sea interface. *J. Phys. Oceanogr.* **4**, 116–120.

HUNT, J. C. R. & SIMPSON, J. E. 1982 Atmospheric boundary layers over non-homogeneous terrain. In *Engineering Meteorology* (ed. E. J. Plate). Elsevier.

ISHII, M. & GROLMES, M. A. 1975 Inception criteria for droplet entrainment in two-phase concurrent film flow. *AIChE J.* **21**, 308–318.

JENSEN, R. J. & YUEN, M. C. 1982 Interphase transport in horizontal stratified co-current flow. *NUREG*/CR-2334, US Nuclear Regulatory Commission, Washington.

KATAOKA, I. & ISHII, M. 1984 Mechanistic modelling of pool entrainment phenomenon. *Intl J. Heat Mass Transfer* **27**, 1999–2014.

KATAOKA, I., ISHII, M. & MISHIMA, K. 1983 Generation and size distribution of droplets in annular two-phase flow. *Trans. ASME* I: *J. Fluids Engng* **105**, 230–238.

KINSMAN, B. 1965 *Wind Waves.* Prentice-Hall.

KITAIGORODSKII, S. A. 1973 *Physics of Air–Sea Interaction.* Israel Program of Scientific Translations, Jerusalem.

KOTAKE, S. 1974 Gas–liquid laminar boundary-layer flows with a wavy phase-changing interface. *Intl J. Heat Mass Transfer* **17**, 885–897.

LAI, R. J. & SHEMDIN, O. H. 1974 Laboratory study of the generation of spray over water. *J. Geophys. Res.* **79**, 3055–3063.

LONGUET-HIGGINS, M. S. 1982 Parametric solutions for breaking waves. *J. Fluid Mech.* **121**, 403–424.

LONGUET-HIGGINS, M. S. 1983 Bubbles, breaking waves and hyperbolic jets at a free surface. *J. Fluid Mech.* **127**, 103–121.

MACHA, J. M. 1981 Modelling the marine ABL including the effects of sea spray. In *Designing with the Wind Symposium, Nantes, June 15–19, 1981*, vol. 1. CSTB.

MONAHAN, E. C. 1968 Sea spray as a function of low elevation wind speed. *J. Geophys. Res.* **73**, 1127–1137.

NAKAGAWA, T. 1983 On characteristics of the water-particle velocity in a plunging breaker. *J. Fluid Mech.* **126**, 251–268.

NEWITT, D. M., DOMBROWSKI, N. & KNELMAN, F. H. 1965 Liquid entrainment: 1. The mechanism of drop formation from gas or vapour bubbles. *Trans. Instn Chem. Engrs* **32**, 244–261.

NIKITIN, I. K. 1972 Approximate calculation of thermally stratified turbulent boundary layer in a region downstream of a sharp change in the roughness of the surface at which flow takes place. *Fluid Mech. Sov. Res.* 1, 177–184.

PAI, S.-I. 1957 *Viscous Flow Theory*, vol. 2. Van Nostrand.

PHILLIPS, O. M. 1977 *The Dynamics of the Upper Ocean*, 2nd edn. Cambridge University Press.

PINCHAK, A. C. 1966 Correlation of some laboratory experiments in two-phase flow with phenomena at the air–sea interface. *USAF Office of Aerospace Res. ARL*-66-0159.

PLATE, E. J. 1978 Wind-generated surface waves: The laboratory evidence. In *Turbulent Fluxes Through the Sea Surface, Wave Dynamics and Prediction* (ed. A. Favre & K. Hasselmann). Plenum.

SCHLICHTING, H. 1960 *Boundary Layer Theory*. McGraw-Hill.

SHAW, C. Y. & LEE, Y. 1976 Wind-induced turbulent heat and mass transfer over large bodies of water. *J. Fluid Mech.* **77**, 645–664.

SINAI, Y. L. 1982 A gross momentum-integral estimate of boundary-layer development over rough water. *24th Brit. Theoret. Mech. Colloquium, City University, London, March 1982.*

SINAI, Y. L. 1983*a* A Charnock-based estimate of interfacial resistance and roughness for internal, fully-developed stratified, two-phase horizontal flow. *Intl J. Multiphase Flow* **9**, 13–19.

SINAI, Y. L. 1983*b* The application of a Charnock-based estimate of interfacial stress to some near-horizontal, stratified two-phase flows. *Thermal-Hydraulics of Nuclear Reactors* (ed. M. Merilo), vol. 1, pp. 226–234. ANS, Lagrange Park.

SINAI, Y. L. 1986*a* An extended Charnock estimate of interfacial stress in stratified two-phase flows. *Intl J. Multiphase Flow* **12**, 839–844.

SINAI, Y. L. 1986*b* Interfacial phenomena of fully-developed, stratified, two-phase flows. *Encyclopedia of Fluid Mechanics*, vol. 3. (ed. N. P. Cheremisinoff), pp. 475–491. Gulf.

SINAI, Y. L. 1986*c* An asymptotic estimate of boundary-layer development over rough water. *Proc. 4th Miami Intl Symp. on Multi-Phase Transport and Particulate Phenomena, 15–17 December 1986, Miami, USA*. Hemisphere.

STREET, R. L. 1979 Turbulent heat and mass transfer across a rough, air–water interface: A simple theory. *Intl J. Heat Mass Transfer* **22**, 885–899.

STREET, R. L., WANG, C. S., MCINTOSH, D. A. & MILLER, A. W. 1978 Fluxes through the boundary layers at an air–water interface; Laboratory studies. In *Turbulent Fluxes Through the Sea Surface, Wave Dynamics and Prediction* (ed. A. Favre & K. Hasselmann). Plenum.

STREETER, V. L. & WYLIE, E. B. 1979 *Fluid Mechanics*. McGraw-Hill Kogakusha, Tokyo.

TENNEKES, H. & LUMLEY, J. L. 1972 *A First Course in Turbulence*. MIT Press.

TOWNSEND, A. A. 1965 Self-preserving flow inside a turbulent boundary layer. *J. Fluid Mech.* **22**, 773–797.

URSELL, F. 1956 Wave generation by wind. In *Surveys in Mechanics*. (ed. G. K. Batchelor & R. M. Davies). Cambridge University Press.

WANG, C. S. & STREET, R. L. 1978 Measurements of spray at an air–water interface. *Dyn. Atmos. Oceans* **2**, 141–152.

WENGEFELD, P. 1978 Impuls, Warme, und Wasserdampf transport an der Oberflache ines offenen Gerinnes Unter dam Einflub des Windes. *Commun. Inst. Hydraul. Engng, University of Karlsruhe* vol. 12.

WOOD, D. H. 1982 Internal boundary layer growth following a step change in surface roughness. *Boundary-Layer Met.* **22**, 241–244.

WU, J. 1968 Laboratory studies of wind–wave interactions. *J. Fluid Mech.* **34**, 91–111.

WU, J. 1973 Spray in the atmospheric surface layer: Laboratory study. *J. Geophys. Res.* **78**, 511–519.

WU, J. 1979 Spray in the atmospheric surface layer: Review and analysis of laboratory and oceanic results. *J. Geophys. Res.* **84**, 1693–1704.

WU, J. 1980 Wind–stress coefficients over sea surface near neutral conditions – a revisit. *J. Phys. Oceanogr.* **10**, 727–740.

WU, J. 1982 Sea spray: A further look. *J. Geophys. Res.* **87**, 8905–8912.

ZANELLI, S. & HANRATTY, T. J. 1971 Relationship of entrainment to wave structure on a liquid film. *Proc. Intl Symp. on Two-Phase Systems, Haifa, Israel, 1971.*